Pharm Res (2013) 30:781–791
DOI 10.1007/s11095-012-0919-x

RESEARCH PAPER

Drug Delivery Characteristics of the Progenitor Bronchial Epithelial Cell Line VA10

Berglind Eva Benediktsdóttir • Ari Jón Arason • Skarphédinn Halldórsson • Thórarinn Gudjónsson • Már Másson • Ólafur Baldursson

Received: 21 June 2012 / Accepted: 18 October 2012 / Published online: 8 November 2012

ABSTRACT

Purpose To determine the integrity and permeability properties of the immortalized human VA10 bronchial epithelial cell line for its suitability as an *in vitro* drug permeation model.

Methods Cells were grown under liquid-covered culture (LCC) or air-liquid interface (ALI) culture, characterized using electron microscopy and immunostaining. Integrity was measured using transepithelial electrical resistance (TER) and permeability of fluorescein sodium (Flu-Na). General permeability was established with dextrans and model drugs and P-glycoprotein (P-gp) function determined with bidirectional flux of rhodamine-123.

Results ALI culture resulted in 2–3 cell layers with differentiation towards ciliated cells but LCC showed undifferentiated morphology. VA10 cells formed TJ, with higher TER in LCC than ALI (~2500 *vs.* ~1200 Ω*cm^2) and Flu-Na permeability ~$1–2 \times 10^{-7}$ cm/s. ALI cultured cells expressed P-gp and distinguished between compounds depending on lipophilicity and size, consistent with previous data from Calu-3 and 16HBE14o-cell lines.

Conclusions ALI cultured cell layers capture the *in vivo*-like phenotype of bronchial epithelium and form functional cell barrier capable of discriminating between compounds depending on physiochemical properties. The VA10 cell line is an important alternative to previously published cell lines and a relevant model to study airway drug delivery *in vitro*.

KEY WORDS air-liquid interface culture · airway permeability · differentiation · drug delivery · human bronchial epithelial cells

ABBREVIATIONS

3D	three-dimensional
A	surface area (cm^2)
A-B	apical-to-basolateral
ALI	air-liquid interface
B-A	basolateral to apical
BSA	bovine serum albumin
CBF	ciliary beating frequency
CFTR	cystic fibrosis transmembrane conductance regulator
FD	fluorescein isothiocyanate labeled dextran
Flu-Na	fluorescein sodium
HBSS	Hanks balanced salt solution
HPV-16	human papilloma virus-16
LCC	liquid-covered culture
NHBE	normal human bronchial epithelial
P_{app}	apparent permeability (cm/s)
PBS	phosphate buffered saline
P-gp	p-glycoprotein
Rb	retinoblastoma tumor suppressor protein
Rh123	rhodamine 123

Electronic supplementary material The online version of this article (doi:10.1007/s11095-012-0919-x) contains supplementary material, which is available to authorized users.

B. E. Benediktsdóttir · M. Másson
Faculty of Pharmaceutical Sciences, School of Health Sciences
University of Iceland, Hofsvallagata 53
107 Reykjavik, Iceland

A. J. Arason · S. Halldórsson · T. Gudjónsson
Stem Cell Research Unit, Biomedical Center
School of Health Sciences, University of Iceland, Vatnsmýrarvegur 16
101 Reykjavik, Iceland

A. J. Arason · T. Gudjónsson
Department of Laboratory Hematology
Landspitali - The National University Hospital of Iceland, Hringbraut
101 Reykjavik, Iceland

S. Halldórsson
Department of Biology, School of Engineering and Natural Sciences
Center for Systems Biology, University of Iceland, Sturlugata 7
101 Reykjavik, Iceland

Ó. Baldursson (✉)
Department of Pulmonary Medicine
Landspitali - The National University Hospital of Iceland
Fossvogur C14
108 Reykjavik, Iceland
e-mail: olafbald@landspitali.is

SEM	scanning electron microscopy
TER	transepithelial electrical resistance (Ω*cm^2)
TJ	tight junction

INTRODUCTION

The airway epithelium is the first physical barrier met by inhaled drugs on their way to potential site of action. To elucidate the fate of these drugs and their interaction with the biological system, it is important to understand the barrier- and permeability characteristics of this region. *In vivo* models are most relevant to study airway drug delivery, however they are less suitable for use at the early stages of drug development (1). *In vitro* cell models have emerged as a more convenient method to study drug permeability due to their relative simplicity and reproducibility. In particular, the use of monolayer epithelial cultures to classify permeability of certain new drugs absorbed in the gastrointestinal tract has been recommended by both the Food and Drug Administration and the European Agency for the Evaluation of Medicinal Products (2,3), thereby highlighting the importance of valid *in vitro* cell models.

Currently, there are only a handful of representative respiratory cell lines that are useful for modeling epithelial integrity and drug permeation (1,4,5). The two cell lines commonly used to study upper airway drug permeation *in vitro* are Calu-3 and 16HBE14o- bronchial epithelial cell lines. Both these cell lines have functional barrier properties (6–8) and their permeability characteristics correlate with *ex vivo* (9) and *in vivo* models (10). Although these cell lines show favorable permeation characteristics, they are different in origin. Calu-3 cells were isolated from adenocarcinoma in the submucosal gland (11) but 16HBE14o- cells were isolated from the second-generation bronchi of a 1-year old heart-lung transplant patient and immortalized with SV40 large T-antigen virus (7). The difference in origin translates into morphological differences between these two cell lines. Calu-3 cells form either a monolayer in culture (6,12,13) or cell layers (14,15) and produce mucus (16,17). Ciliate-like structures have been reported (15) that have been observed to disappear with increasing passage number (18). On the other hand, 16HBE14o-cells show microvilli protrusions, form 1–5 layers of cells when grown in liquid-covered culture (LCC) and 10–16 cell layers in air-liquid interface (ALI) culture (19,20). Investigation of specific events such as drug permeation or host-pathogen interaction requires a cell line that has cell type specificity, morphology and functional integrity relevant to the *in vivo* epithelium. Although the abovementioned cell lines are capable of modeling *ex vivo* or *in vivo* epithelial permeability, there is a need for a cell line that both captures more closely the phenotypic traits of the normal *in vivo* bronchial epithelium and can be used to model drug delivery across the airway epithelium.

We have recently established a human bronchial epithelial cell line, referred to as VA10, by retroviral transfection of constructs containing E6/E7 oncogenes from the human papilloma virus-16 (HPV-16) (21). VA10 has basal- and stem cell phenotype, expressing basal cell markers such as cytokeratins 5/6 and 14 and the basal associated transcription factor p63 (21). The stem cell properties of VA10 are displayed by its ability to form bronchioalveolar-like structures in three-dimensional (3D) co-culture with endothelial cells (22). Furthermore, VA10 generates active tight junctions (TJ) in ALI culture as evidenced by high transepithelial electrical resistance (TER) (21). The fact that VA10 can produce *in vivo* like phenotype in 3D culture and form high TER in ALI makes this cell line a potential candidate for studying bronchial epithelial integrity and response to drug delivery. However, data describing its permeability properties are lacking which is imperative for its acceptance as an *in vitro* airway drug permeation model. For this upper airway epithelial cell line to be considered as a valid model, its properties should reflect the epithelium *in vivo* as closely as possible; discriminating between compounds depending on their lipophilicity, size and transport mechanism and represent the *in vivo* phenotype. The aim of this study was therefore to elucidate the morphological and permeation properties of the VA10 cell line.

MATERIALS AND METHODS

Materials

Atenolol, alprenolol HCl, (±)-metoprolol (+)-tartarate, (±)-propranolol HCl, fluorescein sodium (Flu-Na), fluorescein isothiocyanate labeled dextrans (FD) 4, 10, 20 and 40 kDa, rhodamine 123 (Rh123), terbutaline hemisulfate and verapamil HCl were obtained from Sigma-Aldrich (St. Louis, USA). Mouse monoclonal anti-P-glycoprotein (P-gp, ab3366, clone JSB-1) and mouse monoclonal anti-acetylated tubulin (ab11323, clone 6-11B-1) antibodies were purchased from Abcam (Cambridge, UK), polyclonal rabbit anti-occludin antibody from Zymed (CA, USA) and F-actin phallotoxin, To-Pro-3 and isotype specific Alexa Fluor secondary antibodies were purchased from Invitrogen (Oregon, USA). Fluoromount-G antifade solution was purchased from SouthernBiotech (Birmingham, USA). Cell culture plastics were obtained from Becton Dickinson (NJ, USA). Transwell cell culture filters (pore size 0.4 μm, 12 mm diameter, polyester membrane) were purchased from Corning Costar corporation (through Sigma-Aldrich) and were collagen coated with PureCol® solution from Advanced BioMatrix (CA, USA). Black 96 well microplates were purchased from Eppendorf (Hamburg, Germany). The cell culture medium LHC-9 and

Dulbecco's minimum essential medium:Ham's F12 1:1 (DMEM/F-12) medium were obtained from Gibco (Burlington, Canada) and supplemented with 50 IU/ml penicillin, 50 μg/ml streptomycin and 40 μg/ml azithromycin (Pfizer). Ultroser-G serum substitute was purchased from Pall Life Sciences (Cergy-Saint-Christophe, France).

Culture of the VA10 Bronchial Epithelial Cell Line

The newly established bronchial epithelial cell line, VA10 (21), was used between passages 15–21. The cells were maintained in 75 cm^2 flasks in a humidified incubator at 37°C (5% CO_2) containing bronchial epithelial growth medium (LHC-9). Medium was aspirated and changed every other day with a fresh, prewarmed medium. Transwell filters, used for TER, morphology, and permeability experiments, were collagen coated by applying 0.5 mL of diluted PureCol® (1:44 in phosphate buffered saline, PBS) to each Transwell, that was dried at 37°C and finally rinsed with PBS. Then, the cells were seeded at the density of 2×10^5 cells/cm^2 in the upper chamber of Transwell filters and cultured in LHC-9 medium for 5–6 days, with 0.5 ml medium added to the apical side and 1.5 ml medium to the basolateral side. Subsequently, the cells were cultured in a DMEM/F-12 medium supplemented with 2% Ultroser G with medium changed every other day. For ALI culture, the medium was aspirated after 5 days in LCC from the apical side and filters rinsed with PBS to bring the culture into ALI, having 1.5 ml of DMEM/F-12 medium with 2% Ultroser G medium at the basolateral side.

Transepithelial Electrical Resistance (TER) Measurements

TER of VA10 cell layers was measured with Millicell-ERS volthometer (Millipore, MA, USA) for LCC and ALI cultures. Prewarmed PBS was added to the apical side of ALI cultured cells to be able to measure the TER. The corrected TER value was obtained after subtraction of the background from the cell-free culture insert.

Immunocytochemistry

Cells, cultured at either LCC and ALI until maximum TER was reached, were fixed for 10 min with 3.7% (*v/v*) formaldehyde (after formaldehyde fixation, acetylated tubulin samples were treated with MeOH for 5 min at −20°C), permeabilized with 0.1% (*v/v*) Triton X-100 for 7 min and then blocked (5% *v/v* goat serum, 0.3% *v/v* Triton X-100 in PBS) for 10 min. The following primary antibodies were used: mouse anti-P-gp (IgG_1, 1:30), mouse anti-human acetylated tubulin (IgG_{2b}, 1:700), rabbit anti-human occludin (1:240) and Alexa Fluor 488 phallotoxin for F-actin staining (1:40) and diluted in a buffer consisting of 0.2% (*v/v*) Triton X-100, 0.1% (*w/v*) bovine serum albumin (BSA) and 0.05% (*v/v*) Tween®20 in PBS. Cells were incubated with primary antibodies overnight at 4°C. Then, the cells were incubated with isotype specific Alexa Fluor secondary antibodies (1:1000) and To-Pro-3 for nuclear staining (1:500), diluted with the same solution as for the primary antibodies, for 30 min.

Confocal Microscopy

Immunofluorescence images were obtained using Zeiss LSM 5 Pascal confocal laser scanning microscope (CLSM, Carl Zeiss AG, Munich, Germany) with Plan-Neofluar 40x and Plan-Apochromat 63x oil immersion lenses. VA10 cell layers were mounted with Fluoromount-G and coverslips before visualization.

Scanning Electron Microscopy (SEM)

The VA10 cells were grown on Transwell filters until maximum integrity was reached as determined with TER. Then, the cell layers were washed with PBS, fixed in 3.7% (*v/v*) formaldehyde for 15 min, post-fixed in 1% (*v/v*) OsO_4 for 1 h followed by dehydration through an ethanol gradient of 5, 12.5, 25, 50, 75 and 100% (*v/v*) in water, each step for 10 min at room temperature. The dehydrated cell layers were then transferred in 100% acetone to a critical point drier (Bio-Rad, England). Dried samples were mounted on aluminum stubs and gold sputter-coated (Edwards Sputter Coater S150B, BOC Edwards, MA, USA). Images were obtained on a Zeiss Supra 25 Field Emission Scanning Electron Microscope (FE-SEM, Carl Zeiss AG, Munich, Germany) at 5 kV under high vacuum conditions.

Bright Field Microscopy

Paraffin embedded ALI cultures were stained with hematoxylin and eosin. Imaging was performed using a Leica DMI3000B microscope and Leica DFC310 FX camera.

Permeation Studies

LCC and ALI cultured VA10 cell layers were used in the Flu-Na permeation studies at different time points to determine the function of the paracellular epithelial barrier. All other permeation studies were done on ALI cultured cell layers with TER above 800 **Ω*cm**^{2}. Prior to the permeation studies, the cell layers were washed twice with prewarmed Hanks Balanced Salt Solution (HBSS, 146.94 mM NaCl, 5.37 mM KCl, 0.34 mM Na_2HPO_4, 0.44 mM KH_2PO_4, 1.80 mm $CaCl_2 \times 2H_2O$, 0.81 mM $MgSO_4$, 25 mM $NaHCO_3$, 5.55 mM D-glucose and 25 mM HEPES at pH 7.4) and then allowed to equilibrate in the incubator for 30 min in HBSS (0.5 mL apical and 1.5 mL basolateral). The TER was measured right

before and after the experiment to ensure the integrity of the cell layers. Flu-Na was dissolved in HBSS buffer to a final concentration of 50 μM. FD with average molecular weight of 4, 10, 20 and 40 kDa (FD4, FD10, FD20, FD40) were dissolved in HBSS to a final concentration of 2.5 mg/mL. The model drugs alprenolol, metoprolol, propranolol and terbutaline were prepared in HBSS at final concentration of 100 μM, with atenolol containing 0.1% DMSO and the final concentration of 500 μM.

Before the permeation studies were started, the HBSS buffer was aspirated from the apical surface and replaced by 0.52 mL of prewarmed HBSS test solution, with 1.50 mL of HBSS in the basolateral chamber. Immediately, a sample (20 μL) of the test solution was removed to determine the initial concentration (C_0). The cells were incubated at 37°C and agitated on an orbital shaker at 80 rpm. Sampling from the basolateral compartment (100 μL for Flu-Na and FD, 200 μL for model drugs) was done after 20, 40, 60, 80 and 120 min and replaced with equal volume of fresh HBSS buffer. When the experiment was finished, a sample (20 μL) was removed from the apical chamber to determine drug recovery.

Bidirectional transport studies with the P-gp substrate Rh123 were performed with and without the P-gp efflux pump inhibitor verapamil. Flu-Na was used as a negative control. In studies with verapamil, the cell layers were incubated with verapamil (200 μM) for 1 h prior to the transport experiment. To ensure continued inhibition, verapamil was also present during the Rh123 transport experiment. Apical-to-basolateral (A-B) and basolateral-to-apical (B-A) transport were initiated by adding 0.52 mL or 1.52 mL respectively of either prewarmed Rh123 (50 μM) or Flu-Na (50 μM) to the donor chamber. Sampling (100 μL) from the receiver chamber was as described above.

Sample Analysis

Samples from Flu-Na, FD and Rh123 studies were directly added to black 96 well plates. In Flu-Na and FD studies, 10 mM NaOH aqueous solution (100 μL) was added to each sample. Fluorescence was measured with excitation wavelength of 485 nm and emission of 535 nm using a fluorospectrometer (Tecan GENios microplate reader, Männedorf, Switzerland). Samples from drug permeation studies were analyzed using a Dionex Ultimate 300 HPLC system, coupled with photodiode array detector using Onyx monolithio C18 column (100 mm×4.6 mm). The mobile phase consisted of acetonitrile and H_20/AcOH (99.5/0.5) using conditions described in Table I.

Calculations and Data Analysis

cLogD(7.4) and polar surface area (PSA) were calculated using ChemAxon MarvinSketch software (Budapest, Hungary). Apparent permeability (P_{app}) coefficients were calculated from the permeation experiment according to Eq. 1 where dQ/dt is the flux, A is the surface of the cell filter (1.12 cm^2) and C_o is the initial concentration in donor chamber.

$$P_{app} = \frac{dQ}{dt} \times \frac{1}{C_0 A} \quad (1)$$

All data were reported as mean ± standard deviation with n representing number of experiments. Unpaired, two tailed Student's *t*-test was used to compare two means and one-way analysis of variance (ANOVA) was used to analyze more than two sets of data (GraphPad Software, Inc., CA, USA) with the difference considered to be statistically significant when $p<0.05$.

Table I HPLC Conditions for Model Drugs

Drug	UV detector wavelenght (nm)	Acetonitrile (%)	Flow rate (ml/min)	Retention time (min)
Alprenolol	273	31.5	0.8	2.80
Atenolol	274	7	1.0	2.72
Metoprolol	273	22	0.8	2.81
Propranolol	264	30	1.0	2.57
Terbutaline	274	7	1.0	2.49

RESULTS

Morphological Characterization of VA10 Cell Layers

The epithelial properties of VA10 cells were elucidated with SEM and immunostaining of TJ proteins. VA10 cells were grown on Transwell filters and visualized by SEM, revealing a clear difference between cells cultured under LCC and ALI conditions (Fig. 1a and b). Although both culture conditions generated a confluent cell layer, ALI cultures showed more differentiated cell layers with pronounced ciliated-like protrusions (Fig. 1b). This observation was further supported by the staining of the cilia marker acetylated tubulin (Fig. 1d and e) that was apically located in ALI cultured VA10, showing differentiation towards ciliated epithelial cells. The VA10 cell thickness in ALI culture was 2–3 cell layers (Fig. 1c), showing cuboidal morphology and contact inhibition growth. Both VA10 cells cultured at LCC and ALI expressed the TJ protein occludin that was co-localized with F-actin, forming a highly organized structure (Fig. 2). Expression of these TJ markers indicates a structural barrier that can be functionally monitored with TER.

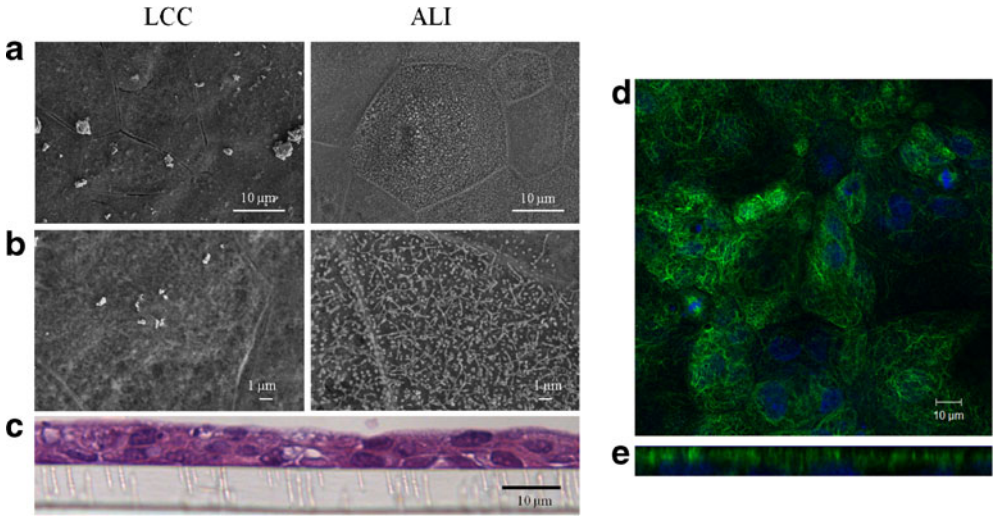

Fig. 1 Morphology of VA10 cell layers. VA10 cells were cultured on Transwell filters before visualization . SEM images (**a**, **b**) of VA10 epithelium cultured in LCC or ALI culture after 21 days in culture. (**c**) Light microscopy image of semithin sections of ALI VA10 cell layers after 25 days in culture. Ciliated differentiation was observed within the ALI cultured epithelium and its thickness was 2–3 cell layers. In contrast, cells grown in LCC generated an undifferentiated phenotype. Immunofluorescent staining of acetylated tubulin (green), a marker for ciliated epithelium, and nuclear staining (blue) in ALI VA10 cell layers, cultured for 22 days, were visualized in confocal microscopy in either regular plane (**d**) or vertical xz cross sections of VA10 cell layer (**e**) showing the apical distribution of acetylated tubulin.

Integrity properties of the VA10 cell layers in LCC and ALI culture

Measurements of TER and permeability for the hydrophilic paracellular marker Flu-Na were determined for both LCC and ALI culture to follow the gradual development of barrier properties in the VA10 cell model. For both LCC and ALI culture, the P_{app} of Flu-Na decreased with increasing TER as shown in Fig. 3. TER values increased above baseline values around day 12 for LCC (Fig. 3a) followed by a decrease in P_{app} for Flu-Na. Between days 18 and 27 in LCC culture, there was no significant difference in P_{app} values for Flu-Na or in TER values ($p > 0.05$) with an average P_{app} value of $1.06 \pm 0.18 \times 10^{-7}$ cm/s and TER of 2481 ± 208 **Ω***cm^2 (Fig. 3a). ALI culture needed longer time to reach TER values above baseline, or 23 days (Fig. 3b). Between days 27 and 48 in culture, P_{app} values of Flu-Na were not significantly different ($p > 0.05$) with an average P_{app} value

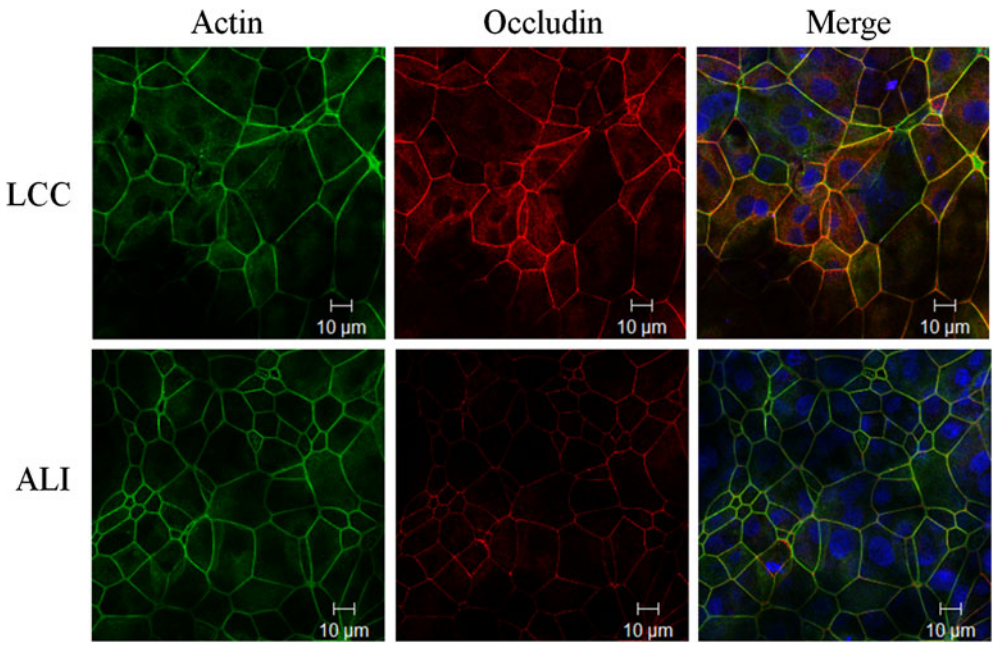

Fig. 2 Tight junction expression in the VA10 cell line grown under LCC or ALI. VA10 cells were cultured on Transwell filters for 22 days. Apical confocal microscopy images were acquired for the tight junction associated protein F-actin (green), the tight junction protein occludin (red), and nucleus (blue).

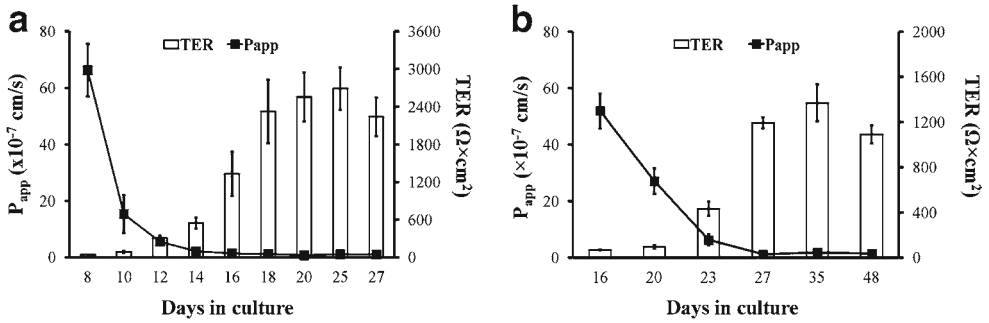

Fig. 3 Epithelial integrity of VA10 cell layers. Transepithelial electrical resistance (TER) and apparent permeability (P_{app}) of Flu-Na for VA10 cell layers, grown on Transwell filters, as a function of time. (**a**) LCC conditions, (**b**) ALI culture conditions. All values are mean ± SD, n=3–5.

of $1.51 \pm 0.33 \times 10^{-7}$ cm/s and TER of 1217±47 Ω*cm^2. Criteria for further permeation studies in ALI was therefore a culture period of ~27 days or TER above 800 Ω*cm^2.

Paracellular Permeability of Dextrans in VA10 Cell Layers

To further investigate the barrier properties of VA10 cell layers, A-B paracellular permeability of Flu-Na and different molecular weight (kDa) FD was investigated in ALI culture (Table II, Fig. 4). Rapid decrease was observed in the P_{app} between Flu-Na and FD10, but a modest decrease in P_{app} values was observed between FD10 and FD40. This inverse proportional relationship between permeation of paracellular markers and their molecular weight confirms that the VA10 model distinguishes between compounds depending on their size.

Drug Permeability in VA10 Cell Layers

Permeability of drugs with different physiochemical properties across ALI cultured VA10 cell layers was determined with four β-adrenoreceptor antagonists (alprenolol, atenolol, metoprolol and propranolol) and one β-adrenoreceptor agonist (bronchodilator, terbutaline). Permeability increased with increased lipophilicity, ranging from $5.21 \pm 0.69 \times 10^{-7}$ cm/s for the hydrophilic atenolol, to $92.87 \pm 6.41 \times 10^{-7}$ cm/s for the lipophilic alprenolol (Table II). A linear relationship (r^2=0.89) was observed between the extent of lipophilicity of the drug at pH 7.4 and its log (P_{app}) value (Fig. 5a). Even stronger relationship was observed between the log (P_{app}) and the PSA of the drugs (r^2=0.96), with decreasing permeability as the PSA increased (Fig. 5b).

Correlation of VA10 Permeability Values with Other *In Vitro* Cell Models

The P_{app} values of compounds with different physiochemical properties obtained in the current study were correlated with previously published P_{app} data from the bronchial epithelial cell lines 16HBE14o- (9) and Calu-3 (10) as shown in Fig. 6. The VA10 permeability data had a strong positive log-linear relationship with both the 16HBE14o- and Calu-3 cell lines (Fig. 6a and b), r^2=0.999 and r^2=0.96 respectively.

Expression of P-glycoprotein

Immunofluorescent staining of the drug efflux P-gp was observed in the VA10 cell layers cultured under ALI (Fig. 7) with the cross section of the cell layer showing

Table II Apical-to-Basolateral P_{app} Values for Compounds Tested in ALI Cultured VA10 Cell Layers

Compounds	MW (Da)	cLogD[a]	PSA[b]	P_{app} ($\times 10^{-7}$ cm/s)[c]	TER (% initial)
Alprenolol	286	0.67	41	92.87 ± 6.41	125
Atenolol	266	−1.73	85	5.21 ± 0.69	133
FD-4	4000	–	–	1.01 ± 0.23	116
FD-10	10000	–	–	0.33 ± 0.13	96
FD-20	20000	–	–	0.29 ± 0.03	84
FD-40	40000	–	–	0.12 ± 0.05	85
Fluorescein-Na	376	−0.77	76	1.51 ± 0.33	105
Metoprolol	685	−0.20	51	69.95 ± 7.92	136
Propranolol	296	0.54	41	62.90 ± 7.33	97
Rhodamine-123	381	0.78	–	3.99 ± 0.57	94
Terbutaline	274	−0.87	73	10.80 ± 3.24	51

[a]cLogD: logarithm of the calculated octanol/water partitioning coefficient at pH 7.4

[b]PSA: molecular polar surface area (Å^2)

[c]Mean ± SD, n=3–5

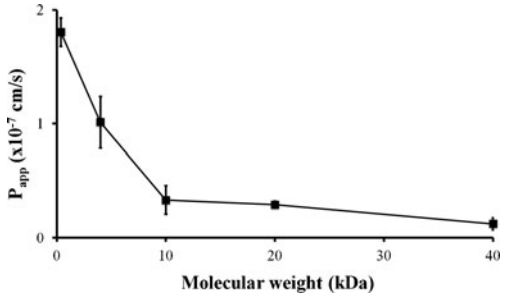

Fig. 4 Paracellular permeability of hydrophilic markers across the VA10 cell layers. P_{app} of Flu-Na and FITC labeled dextrans (FD4, FD10, FD20, FD40) as a function of molecular weight for VA10 cell layers using ALI after 35–37 days in culture. All values are mean ± SD, n=3–4.

predominant apical expression (Fig. 7). No immunofluorescence was observed with the negative control. To confirm the P-gp activity, A-B permeability for the P-gp substrate Rh123 was compared to the B-A permeability (Table III). The P_{app} for Rh123 (50 μM) in the B-A direction was $5.74 \pm 1.16 \times 10^{-7}$ cm/s, compared to $3.99 \pm 0.57 \times 10^{-7}$ cm/s in the A-B direction with the efflux ratio (B-A/A-B) of 1.44. Although the data suggested a trend towards asymmetric transport of Rh123, the difference was not significant ($p > 0.05$). When VA10 cell layers were simultaneously treated with Rh123 and the P-gp inhibitor verapamil (200 μM), the B-A transport of Rh123 decreased by 31% ($p < 0.05$) producing efflux ratio of 1.06, thereby confirming the P-gp mediated efflux of Rh123. P_{app} for the reference compound Flu-Na was symmetric (Table III) and did not change significantly ($p > 0.05$) when treated with verapamil.

DISCUSSION

Epithelial cell lines, immortalized with viral transfection, are suitable to study drug permeation, metabolism and other specific cellular events. In the present study, we have evaluated the epithelial integrity, morphology and permeability properties of the VA10 cell line. The VA10 originates from primary bronchial cells that were transfected with E6 and E7 oncogenes from HPV-16 (21) that targets and inactivates p53 and the retinoblastoma tumor suppressor protein (Rb), respectively. It has been reported in various studies that E6 and E7 immortalized cell lines from organs retain most of the phenotypic traits of their parental cells (23,24). The bronchial epithelial cell line, NuLi-1, was also established by transfection with E6/E7 oncogenes (25). This cell line forms polarized cell layers with established TER and has been proposed as a model to study ion physiology and innate immunity (25). Characterization of this cell line as a permeation model has, however, not been done. Other immortalized bronchial cell lines are available such as the 16HBE14o-cell line (9,26). This cell line has basal cell phenotype (27) and drug permeation values that correlate with reported *ex vivo* data (9). Nevertheless, it forms multiple cell layers consistent with squamous metaplasia when cultured under ALI (19,20) and has limited differentiation potential (20). This compromises the ability of the cell line to model the native bronchial epithelia. Calu-3 is also an established bronchial epithelial cell line. This mucus producing cell line mimics closely the *in vivo* permeability (10), however it does not have the phenotypic traits of normal epithelial cells. Its serous origin in the submucosal glands could have different attributes than its ciliated luminal counterparts (10) and its cancerous origin could lead to different expression levels of metabolizing enzymes (10,18) that raises additional questions to its relevance as a suitable airway epithelial model. Moreover, debates regarding potential cross-contamination or identity of previously established cell lines have emerged (28–30). Therefore, drug evaluation at the cellular level requires the consideration of alternative cell lines.

Using immortalized cell lines where the genotypic alterations are known such as the VA10 cell line is therefore a feasible alternative. The VA10 cell line, which is available from our lab, has a non-malignant phenotype (21) and can capture both bronchial and bronchioalveolar-like epithelial histology, depending on cell culture conditions, thereby showing stem cell properties (22). The cell line expresses basal cell markers such as p63 and cytokeratins 5/6, 13, 14 and 17 when

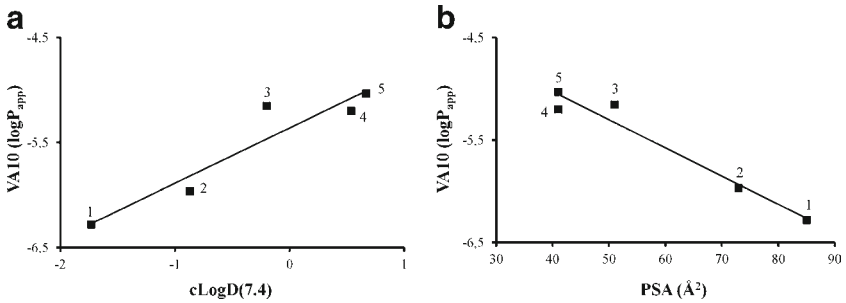

Fig. 5 Correlation of VA10 P_{app}. Drug permeability with their physiochemical properties. Relationship between P_{app} of drugs across ALI cultured VA10 cell layers, cultured for 42 days, with their (**a**) calculated LogD (cLogD) at pH 7.4 (r^2=0.89) and (**b**) with PSA (r^2=96). All values are mean ± SD, n=4. Drug labels: 1-atenolol, 2-terbutaline, 3-metoprolol, 4-propranolol, 5-alprenolol.

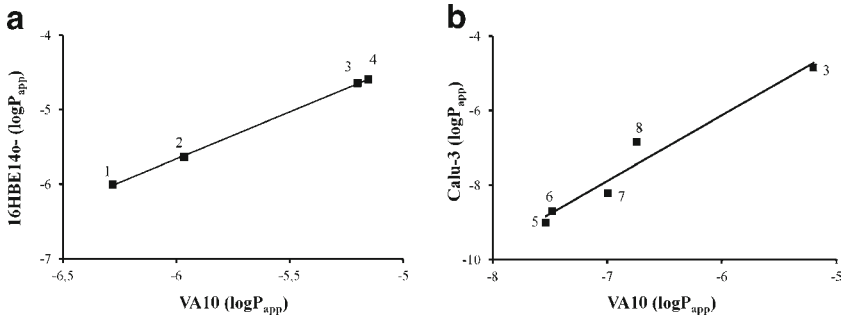

Fig. 6 Correlation of VA10 permeability values to other *in vitro* cell models. Correlation of the apical-to-basolateral P_{app} for various compounds, obtained with ALI cultured VA10 cell layers, with bronchial epithelial cell lines 16HBE14o- (10) (r^2=0.999) (**a**) and Calu-3 (r^2=0.96) (11) (**b**). Each data point represents mean values for each drug. Drug labels: 1-atenolol, 2-terbutaline, 3-propranolol, 4-metoprolol, 5-FD20, 6-FD10, 7-FD4, 8-Flu-Na.

cultured under LCC (21), thus establishing a basal cell phenotype. Basal cells are among the most prominent cell types in the upper airways, occupying ~30% of the cells in the epithelial lining (31) and are considered to be the progenitor cells of mucosal and ciliated epithelial cells (31,32). ALI cultured airway epithelial cells have been described to have a similar gene expression profile as airway epithelial cells *in vivo* (33). We have previously shown that ALI cultured VA10 cells at the basolateral side are p63 positive but cells on the apical side are p63 negative (21) suggesting partial differentiation away from its basal origin. ALI cultured VA10 cells have been shown to stain positive for the cilia markers cystic fibrosis transmembrane conductance regulator (CFTR) and ezrin (34). The current study shows directly the differentiation towards ciliated phenotype, with SEM showing ciliated-like structures and cell layers staining positive for the cilia marker acetylated tubulin (Fig. 1). The ciliated-like structures were not observed under LCC, concurring with previous reports that ALI cultures yield more differentiated phenotype than LCC (35,36). Additionally, under ALI conditions, a part of the VA10 cell culture has been observed to have beating cilia amounting to 6–7 Hz (Supplementary Material). Ciliary beating frequency (CBF) in *ex vivo* cell cultures of ~6 Hz has been reported (37,38) although researchers have also reported CBF of 11–14 Hz (39). Therefore, the differentiation towards ciliated cells in VA10 is evident. Since basal and ciliated cells occupy a large proportion of the bronchial epithelial lining (31), the VA10 cell line can be considered to capture the *in vivo*-like phenotype

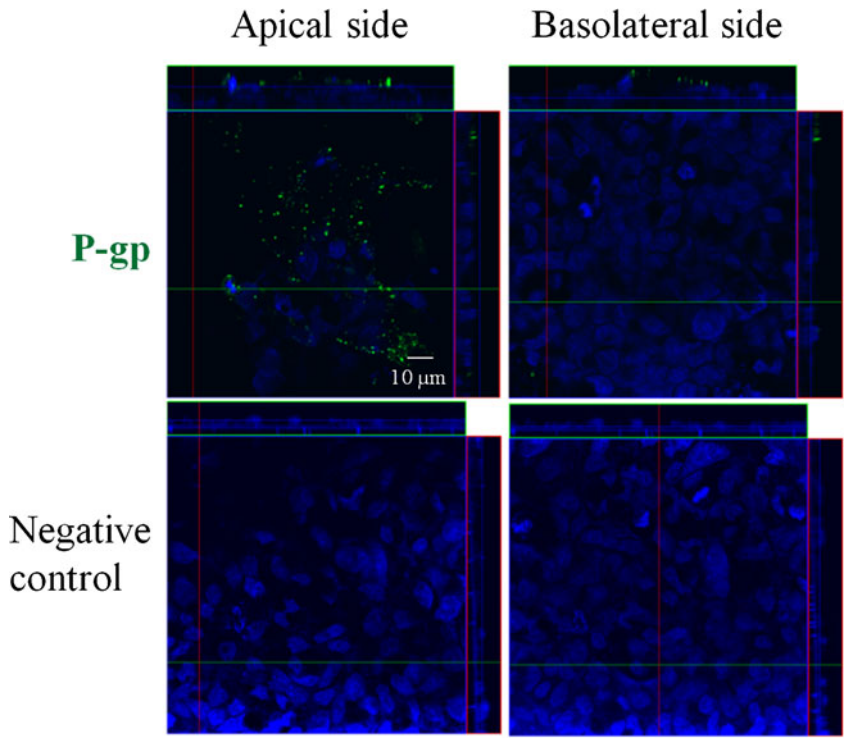

Fig. 7 Localization of P-gp in VA10 epithelium. VA10 cells were cultured under ALI conditions for 34 days. Immunofluorescent localization of P-gp (green), and nucleus (blue) in either regular plane or vertical xz cross sections showing the apical localization of the P-gp protein.

Table III P_{app} Values for Permeation Markers in the Presence or Absence of the P-gp Inhibitor Verapamil in ALI Cultured VA10 Cell Layers

Compounds	± Verapamil	P_{app} ($\times 10^{-7}$ cm/s)[a]	
		A-B	B-A
Rhodamine 123	−	3.99 ± 0.57	5.74 ± 1.16
Rhodamine 123	+	3.73 ± 0.73	3.97 ± 0.45[b]
Fluorescein-Na	−	1.42 ± 0.21	1.67 ± 0.05
Fluorescein-Na	+	1.43 ± 0.06	1.54 ± 0.12

[a] All values are mean ± SD, n=3–5. Cell layers cultured for 49 days

[b] Significantly different ($p < 0.05$) from B-A without verapamil

of the respiratory epithelium. In addition, VA10 cells formed a cell layer, 2–3 cells in thickness, in ALI culture similar to the 2–3 cell layers observed with primary normal human bronchial epithelial (NHBE) cells in co-culture with fibroblasts (20), thereby approaching the physiological pseudostratified airway epithelium. The VA10 cell thickness differs from the cell lines Calu-3 and 16HBE14o- since Calu-3 cells form either a monolayer in culture (6,12,13) or a couple of cell layers (14,15) and 16HBE14o- 10–16 layers (19,20).

The VA10 cell line generates a polarized cell layer, expressing the TJ proteins occludin, JAM-A, Claudin-1, Claudin-4 and ZO-1 (21,40). Therefore, VA10 has been used to model TJ related events under both normal and pathophysiological conditions (34). In the current study, actin and occludin expression was studied, under both ALI and LCC (Fig. 2), with slightly increased staining of occludin in LCC compared to ALI culture. TER, a useful indicator of the functional integrity of the tight junctions (41), reached a peak value for LCC~2600 $\Omega \times cm^2$ compared to a TER of ~1300 $\Omega \times cm^2$ in ALI culture (Fig. 3). Consequently, this difference in TER was dependent on culture conditions, in agreement with data from the Calu-3 (13,15) and 16HBE14o-cell lines (19). The difference in peak TER did not translate into significant difference in P_{app} values for Flu-Na since P_{app} reached a plateau for TER exceeding 1000 $\Omega \times cm^2$. This has been observed for Calu-3 cells where TER over 450 $\Omega \times cm^2$ provided similar P_{app} for Flu-Na (42). TER obtained with ALI cultured VA10 exhibits similar values as primary NHBE cells or 766 ± 154 $\Omega^* cm^2$ (43) and the Calu-3 cell line or 1126 ± 222 $\Omega^* cm^2$, with P_{app} for Flu-Na of 1.47 ± 0.1 $*10^{-7}$ cm/s (10). Although both LCC and ALI conditions provided functional tight junctions, further permeability characteristics were studied in the ALI model due to its abovementioned relevance.

The inverse relationship observed between paracellular permeability of FD and their molecular weight (Fig. 4) is consistent with previously reported studies with Calu-3 (10,15) although individual values were higher in the current study. A number of model drugs that have different physiochemical properties such as degree of lipophilicity and PSA were evaluated in this study. Increased permeation was observed with higher lipophilicity of the drug (Fig. 5a) confirming that passive permeation in VA10 is dependent on lipophilicity, consistent with results from the Calu-3 cell line (10,44). The decreased TER in terbutaline treated filters after sampling cannot be explained. Control experiments, where only TER was measured, excluded the possibility of sampling techniques decreasing the TER. cLogD values were chosen to correlate with P_{app} of the drugs, since cLogD has a stronger correlation to permeability values of model drugs, taking drug charge into account, than cLogP (45). Passive permeability through biological membranes is also influenced by the degree of hydrogen bonding (46). PSA, which is suitable to describe the hydrogen bonding capacity of a drug (47), showed a negative correlation with the permeability data from the VA10 cell line (Fig. 5b). This demonstrates that permeability of drugs through the VA10 cell layer depends on their lipophilic nature and degree of hydrogen bonding. Additionally, correlation of the data with results from previous studies suggests that VA10 has similar permeability characteristics as the 16HBE14o- (9) and Calu-3 (10) cell lines (Fig. 6).

The presence of the drug transporter P-gp, a member of the ATP binding cassette transporter superfamiliy of membrane proteins, was confirmed in the VA10 cell line (Fig. 7). Transporters such as P-gp are responsible for the efflux of many drugs leading to lower than expected therapeutic concentrations (48). The apical expression of P-gp in the VA10 cell line is consistent with the expression in Calu-3 (49), 16HBE14o- (50) and the normal human bronchus (51). However, the efflux ratio of 1.44 reflects relatively low functional activity compared to 16HBE14o-, Calu-3 and the NHBE cells (16,43,50). This difference could be explained by differences in methodology since both culture conditions, time and passage number have been reported to affect the activity of the P-gp efflux protein (52).

The major limitation of our model is its relatively long culture time needed to obtain good barrier properties, compared to Calu-3 and 16HBE14o- cell lines. This can possibly be due to the progenitor nature of VA10 cells, taking longer time to develop functional barrier integrity. Despite the long culture time before full integrity is reached in ALI culture, this integrity can be maintained for as long as 2–3 weeks in culture. Furthermore, VA10 is an important addition to the previously existing cell lines, introducing a basal to ciliated phenotype that does not form multiple cell layers and is not of cancerous origin. This progenitor cell line would be useful to study passive drug permeation, both para- and transcellularly as well as specific intracellular events. In particular, this cell line provides opportunities to investigate the effects of drugs and other compounds on the cellular development and differentiation potential, such as the involvement of transcription

factors and receptors in induced tumor progression, and the effects of possible paracellular permeation enhancers.

CONCLUSIONS

Here we establish that the new bronchial epithelial cell line VA10 generates cell layers with barrier function, permeability characteristics and morphology that closely resemble the native airway epithelium. Therefore, the VA10 cell line is a useful model to study drug delivery *in vitro*.

ACKNOWLEDGMENTS AND DISCLOSURES

Financial support from the Eimskip Fund of University of Iceland, the University of Iceland Research Fund, the Landspitali University Hospital Science Fund and the Bergthóru and Thorsteins Scheving Thorsteinssonar Fund is gratefully acknowledged. We thank Professor Magnus Karl Magnusson for critical discussion and good advice, Sigrún Kristjánsdóttir at the Pathology Department of Landspitali University Hospital for her contribution to the paraffin prepared samples and Bergthóra S. Snorradóttir at the University of Iceland for help with the HPLC.

REFERENCES

1. Sakagami M. *In vivo*, *in vitro* and *ex vivo* models to assess pulmonary absorption and disposition of inhaled therapeutics for systemic delivery. Adv Drug Delivery Rev. 2006;58(9–10):1030–60.
2. Guidance for industry: Waiver of *in vivo* bioavailability and bioequivalence studies for immediate-release solid oral dosage forms based on a biopharmaceutics classification system. August 2000, CDER/FDA.
3. Note for guidance on the investigation of bioavailability and bioequivalence. December 2000, EMEA.
4. Forbes B, Ehrhardt C. Human respiratory epithelial cell culture for drug delivery applications. Eur J Pharm Biopharm. 2005;60(2):193–205.
5. Sporty JL, Horalkova L, Ehrhardt C. *In vitro* cell culture models for the assessment of pulmonary drug disposition. Expert Opin Drug Metab Toxicol. 2008;4(4):333–45.
6. Shen BQ, Finkbeiner WE, Wine JJ, Mrsny RJ, Widdicombe JH. Calu-3: a human airway epithelial cell line that shows cAMP-dependent Cl- secretion. Am J Physiol Lung Cell Mol Physiol. 1994;266(5):L493–501.
7. Cozens AL, Yezzi MJ, Kunzelmann K, Ohrui T, Chin L, Eng K, *et al.* CFTR expression and chloride secretion in polarized immortal human bronchial epithelial cells. Am J Respir Cell Mol Biol. 1994;10(1):38–47.
8. Wan H, Winton H, Soeller C, Stewart G, Thompson P, Gruenert D, *et al.* Tight junction properties of the immortalized human bronchial epithelial cell lines Calu-3 and 16HBE14o. Eur Respir J. 2000;15(6):1058–68.
9. Manford F, Tronde A, Jeppsson A-B, Patel N, Johansson F, Forbes B. Drug permeability in 16HBE14o- airway cell layers correlates with absorption from the isolated perfused rat lung. Eur J Pharm Sci. 2005;26(5):414–20.
10. Mathias NR, Timoszyk J, Stetsko PI, Megill JR, Smith RL, Wall DA. Permeability characteristics of Calu-3 human bronchial epithelial cells: *In vitro-in vivo* correlation to predict lung absorption in rats. J Drug Target. 2002;10(1):31–40.
11. Fogh J, Fogh JM, Orfeo T. 127 Cultured human tumor-cell lines producing tumors in nude mice. J Natl Cancer Inst. 1977;59(1):221–6.
12. Florea BI, Cassara ML, Junginger HE, Borchard G. Drug transport and metabolism characteristics of the human airway epithelial cell line Calu-3. J Control Release. 2003;87(1–3):131–8.
13. Fiegel J, Ehrhardt C, Schaefer UF, Lehr C-M, Hanes J. Large porous particle impingement on lung epithelial cell monolayers—Toward improved particle characterization in the lung. Pharm Res. 2003;20(5):788–96.
14. Stentebjerg-Andersen A, Notlevsen IV, Brodin B, Nielsen CU. Calu-3 cells grown under AIC and LCC conditions: Implications for dipeptide uptake and transepithelial transport of substances. Eur J Pharm Biopharm. 2011;78(1):19–26.
15. Grainger C, Greenwell L, Lockley D, Martin G, Forbes B. Culture of Calu-3 cells at the air interface provides a representative model of the airway epithelial barrier. Pharm Res. 2006;23(7):1482–90.
16. Haghi M, Young PM, Traini D, Jaiswal R, Gong J, Bebawy M. Time- and passage-dependent characteristics of a Calu-3 respiratory epithelial cell model. Drug Dev Ind Pharm. 2010;36(10):1207–14.
17. Finkbeiner WE, Carrier SD, Teresi CE. Reverse transcription-polymerase chain reaction (RT-PCR) phenotypic analysis of cell cultures of human tracheal epithelium, tracheobronchial glands, and lung carcinomas. Am J Respir Cell Mol Biol. 1993;9(5):547–56.
18. Ehrhardt C, Forbes B, Kim K-J. *In vitro* models of the tracheobronchial epithelium. In: Ehrhardt C, Kim K-J, editors. Drug absorption studies: *in situ*, *in vitro* and *in silico* models. New York: Springer US; 2008. p. 235–57.
19. Ehrhardt C, Kneuer C, Fiegel J, Hanes J, Schaefer U, Kim K-J, *et al.* Influence of apical fluid volume on the development of functional intercellular junctions in the human epithelial cell line 16HBE14o- implications for the use of this cell line as an *in vitro* model for bronchial drug absorption studies. Cell Tissue Res. 2002;308(3):391–400.
20. Pohl C, Hermanns MI, Uboldi C, Bock M, Fuchs S, Dei-Anang J, *et al.* Barrier functions and paracellular integrity in human cell culture models of the proximal respiratory unit. Eur J Pharm Biopharm. 2009;72(2):339–49.
21. Halldorsson S, Asgrimsson V, Axelsson I, Gudmundsson GH, Steinarsdottir M, Baldursson O, *et al.* Differentiation potential of a basal epithelial cell line established from human bronchial explant. In Vitro Cell Dev Biol Anim. 2007;43(8–9):283–9.
22. Franzdottir S, Axelsson I, Arason A, Baldursson O, Gudjonsson T, Magnusson M. Airway branching morphogenesis in three dimensional culture. Respir Res. 2010;11(1):162.
23. Gudjonsson T, Villadsen R, Nielsen HL, Rønnov-Jessen L, Bissell MJ, Petersen OW. Isolation, immortalization, and characterization of a human breast epithelial cell line with stem cell properties. Genes Dev. 2002;16(6):693–706.
24. Gudjonsson T, Villadsen R, Rønnov-Jessen L, Petersen OW. Immortalization protocols used in cell culture models of human breast morphogenesis. Cell Mol Life Sci. 2004;61(19):2523–34.
25. Zabner J, Karp P, Seiler M, Phillips SL, Mitchell CJ, Saavedra M, *et al.* Development of cystic fibrosis and noncystic fibrosis airway cell lines. Am J Physiol Lung Cell Mol Physiol. 2003;284(5):L844–54.
26. Forbes B, Shah A, Martin GP, Lansley AB. The human bronchial epithelial cell line 16HBE14o-as a model system of the airways for studying drug transport. Int J Pharm. 2003;257(1–2):161–7.
27. Dorscheid D, Conforti A, Hamann K, Rabe K, White S. Characterization of cell surface lectin-binding patterns of human airway epithelium. Histochem J. 1999;31(3):145–51.

28. Rojas A, Gonzalez I, Figueroa H. Cell line cross-contamination in biomedical research: a call to prevent unawareness. Acta Pharmacol Sin. 2008;29(7):877–80.
29. Nardone R. Eradication of cross-contaminated cell lines: a call for action. Cell Biol Toxicol. 2007;23(6):367–72.
30. Otton A. Cell culture forensics of Calu-3: a human lung epithelial cell line. Ethn Dis. 2009;19(2):S78–9.
31. Boers JE, Ambergen AW, Thunnissen FBJM. Number and proliferation of basal and parabasal cells in normal human airway epithelium. Am J Respir Crit Care Med. 1998;157(6):2000–6.
32. Rock JR, Onaitis MW, Rawlins EL, Lu Y, Clark CP, Xue Y, *et al.* Basal cells as stem cells of the mouse trachea and human airway epithelium. Proc Natl Acad Sci. 2009;106(31):12771–5.
33. Dvorak A, Tilley AE, Shaykhiev R, Wang R, Crystal RG. Do airway epithelium air–liquid cultures represent the *in vivo* airway epithelium transcriptome? Am J Respir Cell Mol Biol. 2011;44(4):465–73.
34. Halldorsson S, Gudjonsson T, Gottfredsson M, Singh PK, Gudmundsson GH, Baldursson O. Azithromycin maintains airway epithelial integrity during pseudomonas aeruginosa infection. Am J Respir Cell Mol Biol. 2010;42(1):62–8.
35. Mathias NR, Kim K-J, Robison TW, Lee VHL. Development and characterization of rabbit tracheal epithelial cell monolayer models for drug transport studies. Pharm Res. 1995;12(10):1499–505.
36. Yamaya M, Finkbeiner WE, Chun SY, Widdicombe JH. Differentiated structure and function of cultures from human tracheal epithelium. Am J Physiol Lung Cell Mol Physiol. 1992;262(6):L713–24.
37. Clary-Meinesz C, Mouroux J, Huitorel P, Cosson J, Schoevaert D, Blaive B. Ciliary beat frequency in human bronchi and bronchioles. CHEST J. 1997;111(3):692–7.
38. Clary-Meinesz C, Mouroux J, Cosson J, Huitorel P, Blaive B. Influence of external pH on ciliary beat frequency in human bronchi and bronchioles. Eur Respir J. 1998;11(2):330–3.
39. Rutland J, Griffin WM, Cole PJ. Human ciliary beat frequency in epithelium from intrathoracic and extrathoracic airways. Am Rev Respir Dis. 1982;125(1):100–5.
40. Asgrimsson V, Gudjonsson T, Gudmundsson GH, Baldursson O. Novel effects of azithromycin on tight junction proteins in human airway epithelia. Antimicrob Agents Chemother. 2006;50(5):1805–12.
41. Kim K-J. Bioelectrical characterization of cultured epithelial cell (mono)layers and excised tissues. In: Lehr CM, editor. Cell culture models of biological barriers. CRC Press; 2002. p. 41–51.
42. Ehrhardt C, Fiegel J, Fuchs S, Abu-Dahab R, Schaefer UF, Hanes J, *et al.* Drug absorption by the respiratory mucosa: cell culture models and particulate drug carriers. J Aerosol Med. 2002;15(2):131–9.
43. Lin H, Li H, Cho H-J, Bian S, Roh H-J, Lee M-K, *et al.* Air-liquid interface (ALI) culture of human bronchial epithelial cell monolayers as an *in vitro* model for airway drug transport studies. J Pharm Sci. 2007;96(2):341–50.
44. Foster KA, Avery ML, Yazdanian M, Audus KL. Characterization of the Calu-3 cell line as a tool to screen pulmonary drug delivery. Int J Pharm. 2000;208(1–2):1–11.
45. Tronde A, Norden B, Jeppsson AB, Brunmark P, Nilsson E, Lennernas H, *et al.* Drug absorption from the isolated perfused rat lung-correlations with drug physicochemical properties and epithelial permeability. J Drug Target. 2003;11(1):61–74.
46. Conradi RA, Burton PS, Borchardt RT. Physico-chemical and biological factors that influence a drug's cellular permeability by passive diffusion. In: Pliška V, Testa B, van de Waterbeemd H, editors. Lipophilicity in drug action and toxicology. Weinheim: Wiley-VCH Verlag GmbH; 2008. p. 233–52.
47. Clark DE. Rapid calculation of polar molecular surface area and its application to the prediction of transport phenomena. 1. Prediction of intestinal absorption. J Pharm Sci. 1999;88(8):807–14.
48. Balimane PV, Han YH, Chong SH. Current industrial practices of assessing permeability and P-glycoprotein interaction. AAPS J. 2006;8(1):E1–E13.
49. Hamilton KO, Topp E, Makagiansar I, Siahaan T, Yazdanian M, Audus KL. Multidrug resistance-associated protein-1 functional activity in Calu-3 cells. J Pharmacol Exp Ther. 2001;298 (3):1199–205.
50. Ehrhardt C, Kneuer C, Laue M, Schaefer UF, Kim K-J, Lehr C-M. 16HBE14o-human bronchial epithelial cell layers express P-glycoprotein, lung resistance-related protein, and caveolin-1. Pharm Res. 2003;20(4):545–51.
51. Lechapt-Zalcman E, Hurbain I, Lacave R, Commo F, Urban T, Antoine M, *et al.* MDR1-Pgp 170 expression in human bronchus. Eur Respir J. 1997;10(8):1837–43.
52. Madlova M, Bosquillon C, Asker D, Dolezal P, Forbes B. *In-vitro* respiratory drug absorption models possess nominal functional P-glycoprotein activity. J Pharm Pharmacol. 2009;61(3):293–301.